Nanoporous gold obtained from a metallic glass precursor used as substrate for surface-enhanced Raman scattering

This is the author's manuscript

Original Citation:

Availability:

This version is available http://hdl.handle.net/2318/1532255   since   2015-12-30T16:04:34Z

Published version:

DOI:10.1080/09500839.2015.1093665

Terms of use:

Open Access

(Article begins on next page)

07 July 2024

Nanoporous gold obtained from a metallic glass precursor used as substrate for surface-enhanced Raman scattering

F. Scaglione, E.M. Paschalidou, P. Rizzi, S. Bordiga & L. Battezzati

F. Scaglione*, E.M. Paschalidou, P. Rizzi, S. Bordiga and L. Battezzati

Dipartimento di Chimica and Centro Interdipartimentale NIS (Nanostructured Interfaces and Surfaces), Università di Torino, V. Giuria 7, Torino 10125, Italy

Nanoporous gold (NPG) has been synthesized by electrochemical de-alloying a new precursor, amorphous $Au_{30}Cu_{38}Ag_7Pd_5Si_{20}$ (at.%), starting from melt-spun ribbons. Ligaments ranging from 75 to 210 nm depending on the de-alloying time were obtained. Analytical and electrochemical evidence showed the ligaments contain residual Cu, Ag and Pd. Surface-

enhanced Raman scattering from the NPG was investigated using pyridine and 4,4′-bi-pyridine as probe molecules. It was found that the activity is at maximum when the ribbon is fully de-alloyed although the ligaments then have a larger size. The enhancement is attributed to the small size of crystals in the ligaments, to their morphology and to trapped atoms.

1. Introduction

Nanoporous metals obtained by selective removal of less-noble elements from an alloy have various possible applications in catalysis [1], energy conversion [2], actuators [3] and surface-enhanced Raman scattering (SERS) [4]. SERS probes the plasmonic vibration of molecules adsorbed on a suitable substrate [5–8] with mechanisms dependent on the shape [9] and size [10–12] of the substrate at the nanoscale and on its composition [13]. The sensitivity of the technique to active species can approach the detection of single molecules [14,15].

Various substrates have been tested for one-time use in SERS. Dispersed [16–18], colloidal [19] and aggregated nanoparticles [20] point to fast synthesis, shape design [21] and the possibility of functionalization [22]. Larger substrates, which could possibly be reused, have been made by etching Au alloys (e.g. Ag–Au) obtaining so-called nanoporous gold (NPG) [15,23,24], and by anodic roughening Au films [25,26]. De-alloyed NPG is made of interconnected pores and ligaments that contain residual Ag which helps signal enhancement [1]. These materials have still the drawback that ligaments coarsen during processing [27] with consequent deterioration of SERS activity [26,28]. In relation to the present work, it is worth mentioning that the enhancement of the signal is believed to arise from an electromagnetic effect associated with excitation of surface plasmons. In addition, a short-range chemical effect caused by charge transfer

*Corresponding author. Email: federico.scaglione@unito.it

between the adsorbed molecules and the metallic rough substrate can occur as well as polarization on strongly interacting nanostructures [29].

Crystalline alloys retain their starting microstructure on leaching: each grain becomes a porous single crystal [30]. On the contrary, numerous fine crystals of the most stable crystalline structure are produced from metallic glasses [31]. In both cases, the remaining noble atoms move by surface diffusion. The network of ligaments is formed epitaxially in crystalline alloys and by impingement of nanocrystals in the latter case [32]. Since complex composition is a requirement for glass-forming ability, the likelihood of less-noble atoms being incorporated as impurity in the newly formed crystals is maintained [33]. Finally, the products of rapid quenching the melt are thin ribbons, which remain free standing after de-alloying. With this background, we explore the chance of employing NPG obtained by electrochemical de-alloying an amorphous precursor, $Au_{30}Cu_{38}Ag_7Pd_5Si_{20}$ (at.%), as a reusable substrate for SERS using pyridine and 4,4′-bipyridine as probe molecules.

2. Experimental details

A $Au_{30}Cu_{38}Ag_7Pd_5Si_{20}$ (at.%) ingot was prepared by arc-melting lumps of pure elements in a Ti-gettered Ar atmosphere. Ribbons 25 μm thick and 2 mm wide were made by melt spinning the master alloy onto a copper wheel in a closed chamber kept under

Ar. Samples of 15 mm in length were cut for de-alloying. The structure and microstructure of samples were studied by X-ray diffraction (XRD) in Bragg–Brentano geometry with monochromatic Cu-K$_\alpha$ radiation, and by scanning electron microscopy (SEM) with energy dispersive X-ray spectroscopy (EDS) before and after etching.

Polarization experiments with a scan rate of 5 mV/s were performed with as-spun ribbons in 1 M HNO$_3$ aqueous solution in a three-electrode cell (saturated Ag/AgCl double-bridge reference electrode, Pt counter electrode and the sample as working electrode) at the temperature of 70 °C chosen to increase the rate of dissolution; the corrosion potential is 0.56 V. The anodic current density reaches a maximum value of about 10^{-3} A/cm^2 at 1 V followed by a passivation region (1.1 V to 1.5 V) with a lower current density of 10^{-4} A/cm^2, and trans-passivation. The potential for de-alloying was then set to 1 V. At this potential, the current density reached 10^{-3} A/cm^2 in about 2000s during which possible surface passive layers were removed and de-alloying began. Then the current remained steady for some hours until it finally decreased smoothly to a background level.

Micro-Raman measurements were performed with a Renishaw inVia Raman microscope using 785-nm laser line, 1% power at the sample and a 20 × ULWD objective. Samples were cleaned in concentrated ammonia hydroxide and rinsed several times in deionized water before experiments. Pyridine (py) and 4,4′-bipyridine (bipy) were chosen as SERS probe molecules because their adsorption properties are well characterized in the literature [16]. All solutions were prepared from chemical grade reagents and deionized water.

3. Results and discussion

The composition Au$_{30}$Cu$_{38}$Ag$_7$Pd$_5$Si$_{20}$ (at.%) has been newly devised with lower Au content with respect to previous reports [29] for easier de-alloying. Rapidly quenched

ribbons resulted in fully amorphous samples as determined by XRD (Figure 1) and no composition inhomogeneity was detected by extensive EDS analyses. The glass transition and crystallization temperatures of the samples occur at 168 and 190 °C, respectively, on heating at 20 K/min.

3.1. Structure, microstructure and composition of de-alloyed samples

Figure 1 displays a series of XRD patterns, showing that, with the progress of etching, the intensity of the amorphous halo is lowered and reflections arising from randomly distributed crystals of a face-centred cubic (f.c.c.) phase develop. Lattice constants of all samples are close to that of Au within the experimental error. The reflections are broad, indicating that the ligaments contain fine scattering domains with sizes of 30 nm (de-alloying up to one hour), 50 nm (three hours) and 70 nm (six hours and more) from Rietveld refinement.

The morphology of the samples during de-alloying is shown in the SEM images of Figure 2a–d: channels and irregular rafts first appear and progressively develop into pores and ligaments across the thickness. The ligaments contain grain boundaries, often recognized by the appearance of grooves on the external surface, resulting from impingement of crystals that have grown independently. The size of ligaments measured at their narrower necks increases as a function of de-alloying time for the first 200 min from 75 (below one hour) to 210 nm; then, it remains constant for longer times within the accuracy that can be reached in their measurement (Figure 2e). Since the de-alloying proceeds from both sides, a dividing line in the middle of the ribbon appears at the end of the process as seen in Figure 2d.

After de-alloying for 15 min, EDS reveals the ribbon contains Au as main constituent with reduced quantities of the other elements – all sampled in crystalline protrusions and also in the still amorphous portion. The Si content is 7 at.% entirely contained in the glassy phase. The Cu content is 28 at.%, in excess with respect to the
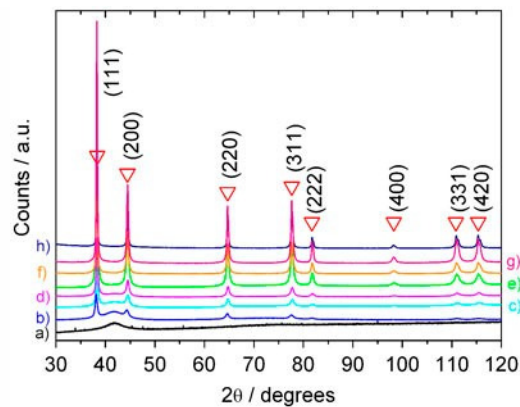

Figure 1. XRD patterns of (a) the as-spun $Au_{30}Cu_{38}Ag_7Pd_5Si_{20}$ (at.%) ribbon and samples de-alloyed for (b) 10 min, (c) 15 min, (d) 30 min, (e) 1 h, (f) 2 h, (g) 4 h and (h) 6 h; $\triangledown$ Au reflections.
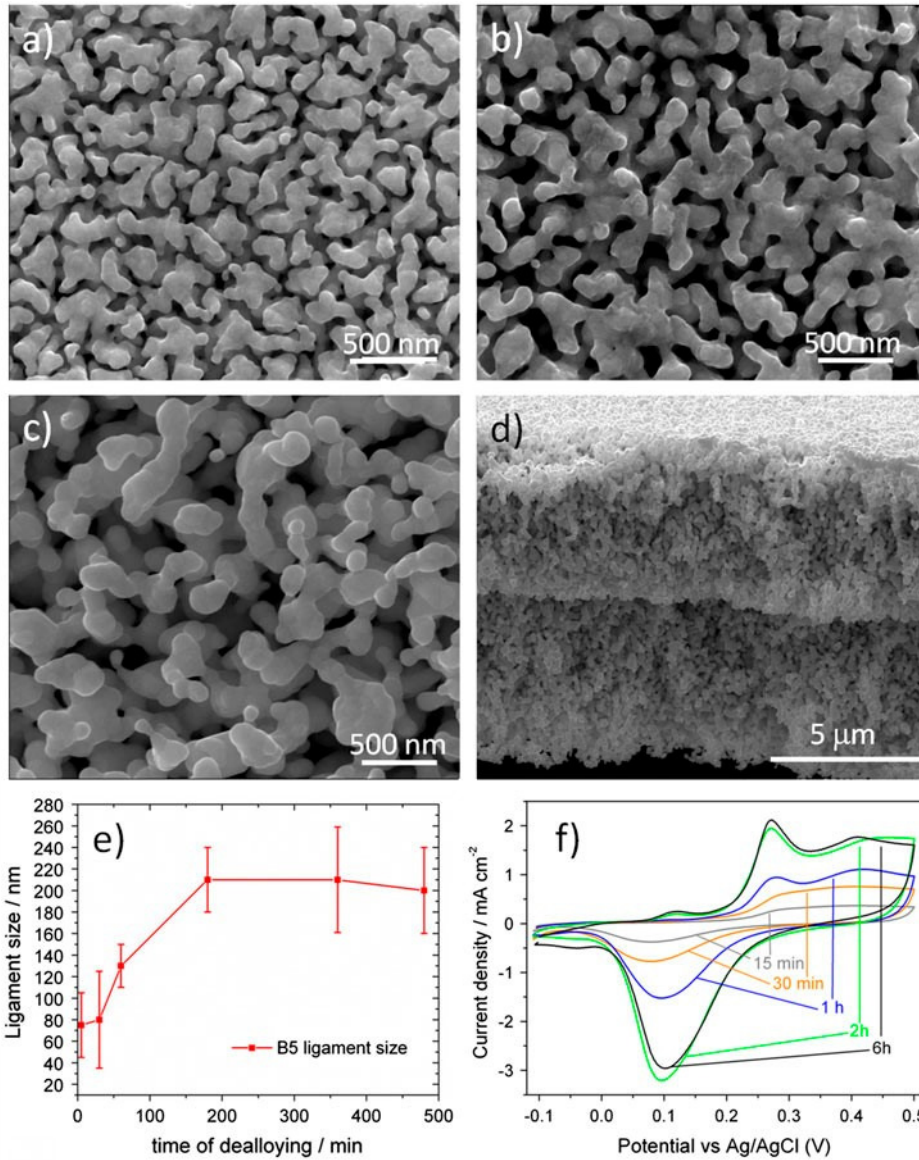
Figure 2. SEM images of surfaces of samples de-alloyed for (a) 30 min, (b) 2 h, (c) 6 h and (d) cross section of the 6-h sample. (e) Size of ligaments as a function of de-alloying time measured at the narrower neck of at least 100 ligaments. Scatter bars represent two standard deviations of the size. (f) Cyclic voltammetry scans of ribbons de-alloyed for the times listed in the legend.

ratio to Si in the metallic glass, and so must be contained both in the ligaments and the glass. The Ag and Pd contents of 2.3 at.% and 1.3 at.%, respectively, are also contributed by both phases. These values are indicative since they are associated with a scatter of about 30%. It is concluded, however, that Cu, Ag and Pd remain trapped in

the crystals. In the sample de-alloyed for 30 min, Si, Ag and Pd are detected only at isolated places, while Cu is still found at 7 at.%. After longer etching, the less-noble metals were found occasionally in measurable quantity; however, inspection of the spectra revealed traces of Pd and Ag although their amounts could not be quantified. A signature of the presence of Ag and Pd in ligaments was obtained with cyclic voltammetry performed in KOH (Figure 2f). The literature shows that formation of Ag_2O and AgO is marked by current peaks starting around 0.30 V on the forward scan and 0.25 V on the backward scan [34]. In the present samples, this range is partly overlapped by the strong signal arising from the formation of oxides of nanoporous Au beginning at 0.20 V [34]. However, the signals above 0.35 V, well apparent for samples de-alloyed for at least 1 h, indicate the occurrence of residual Ag on the surface. Moreover, the small current peak detected around 0.06 V can be attributed to the oxidation of surface Pd atoms [35–37].

3.2. SERS experiments

The Raman-enhancing capability of ribbons de-alloyed for different times was tested after immersing the samples in 5 ml of solution of pyridine in water. Figure 3A shows spectra acquired at random on both sides of a ribbon de-alloyed for 6 h: although the relevant absorption bands are clearly present, the intensity differs from point to point indicating that the active sites are not homogeneously distributed on the surface and that their number is limited. Figure 3B shows the strongest signal collected with samples de-alloyed for different times, and having ligaments and pores of different sizes. The strongest activity
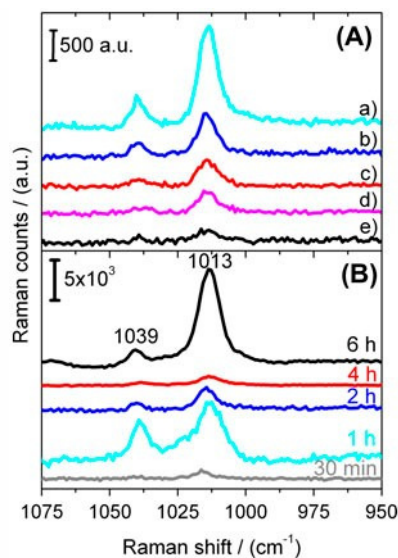

Figure 3. (A) SERS spectra of 10^{-3} M pyridine on a ribbon de-alloyed for 6 h; letters (a) to (e) refer to spectra acquired at random on the surface of the ribbon. The spectra are shown here with increasing intensity for clarity of presentation, not in the order of recording. (B) SERS spectra of 10^{-3} M pyridine on ribbons at different time of de-alloying.

occurs for the sample de-alloyed for 6 h, which is fully de-alloyed and has coarser microstructure. It is surprising that all these samples are SERS active since their microstructural features do not reach the size expected for the effect to occur, namely a few tens of nanometres at maximum [26–28]. The positive SERS response must then be attributed to other causes. It is apparent in the images of Figure 2 that the local curvature of ligaments (and of pores in between them) is small enough at some places for the ligament walls to be located at very short distances from other walls, compatible with the excitation of 'hot spots'. Additionally, crystal defects intersect the surface and cause roughening. Recalling that the crystals contain small amounts of Ag and Pd, it is believed that their presence, especially Ag, favours the SERS effect as shown in the case of a de-alloyed Ag–Au alloy [13]. The fully de-alloyed ribbon was also found to display better electrocatalytic activity with respect to methanol oxidation. This could be attributed to the poisoning of Au(Ag) active sites by oxidized Cu which continues to be released from the underlying amorphous alloy during the etching process [32]. The role of Cu, a plasmonic metal, must then be clarified with respect to the SERS activity. De-alloyed porous Cu, free from surface oxide, was active for SERS using rhodamine 6G as model molecule [38], whereas copper oxides were shown to be active when interacting with molecules containing specific moieties, e.g. thiol [39] and acid [40] groups. It is concluded that the simultaneous presence of zero-valent (Au, Ag) and oxidized (Cu) elements on the ligaments surface is detrimental to the SERS activity of our samples, which is enhanced when the oxides are removed.

Since the polycrystalline ligaments, made of various crystals with interfaces in between, and their morphology are supposed to play a role in the activity of the porous gold derived from a metallic glass, a material was produced for comparison by leaching ribbons of a $Au_{31}Cu_{41}Zn_{12.8}Mn_{15.2}$ (at.%) crystalline alloy known to be single-phased f.c.c. [41]. The ribbon is constituted of columnar grains, several micrometres in size and retains the original microstructure after etching. The resulting ligaments are part of large porous single crystals in contrast to the grooved ones obtained with the amorphous precursor. They are, however, of similar size in both materials. This sample did not display SERS activity even when fully de-alloyed, that is, Cu free. The combined
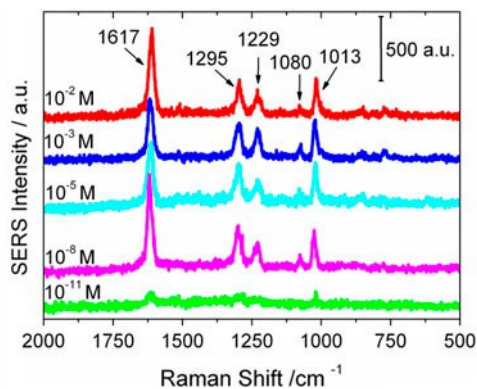

Figure 4. SERS spectra of 4,4′-bipyridine at different concentration in ethanol on ribbons de-alloyed for 6 h.

effect of impurity atoms, Ag and possibly Pd, combined with the shape and microstructure of the ligaments, appears to cause the SERS enhancement in fully de-alloyed ribbons made from amorphous precursors.

Ribbons de-alloyed for 6 h were selected for further investigation by immersing them for 5 min in an ethanol solution of the probe molecule bipyridine at concentrations from 10^{-2} to 10^{-11} M and then dried in air. The Raman spectra shown in Figure 4 are the most intense ones among the 10 collected for each concentration at the low beam power of 0.05%, which was preferred to avoid heating. The observed peak positions are in good agreement with data from the literature [42]. The intensity of peaks does not appear to be affected by concentrations in the range from 10^{-2} to 10^{-8} M but decreases at the 10^{-11} M concentration. This is compatible with a saturation effect of 'hot spots'. The substrate then becomes sensitive to adsorbed molecules in low concentration and can be reused after proper washing.

4. Conclusions

In this Letter, the production and characterization of NPG ribbons with tuneable size of ligaments and pores as a function of de-alloying time is reported. Their SERS activity does not depend on the ligament size but is a maximum when the sample is de-alloyed through the entire thickness, although this then contains the largest ligaments. This has been attributed to the combined effect of the local composition of ligaments, which retain randomly distributed atoms of Ag and Pd, of the small size of crystals in the ligaments, and of ligament shape. Although the SERS effect is not constant across the NPG surface, enhancement is significant, reaching a sensitivity up to 10^{-11} M.

Disclosure statement
No potential conflict of interest was reported by the authors.

References

[1] X.Y. Lang, H. Guo, L.Y. Chen, A. Kudo, J.S. Yu, W. Zhang, A. Inoue and M.W. Chen, J. Phys. Chem. C 114 (2010) p.2600.
[2] H.J. Qiu, H.T. Xu, L. Liu and Y. Wang, Nanoscale 7 (2015) p.386.
[3] H.J. Jin and J. Weissmüller, Adv. Eng. Mater. 12 (2010) p.714.
[4] H. Min, N. Sullivan, D. Allara and S. Tadigadapa, Procedia Eng. 25 (2011) p.1469.
[5] M. Moskovitz, Rev. Mod. Phys. 57 (1985) p.783.

[6] J.A. Creighton, Surf. Sci. 124 (1983) p.209.

[7] D.H. Jeong, Y.X. Zhang and M. Moskovitz, J. Phys. Chem. B 108 (2004) p.12724.

[8] M. Baibarac, I. Baltog, S. Lefrant, J.Y. Mevellec and O. Chauvet, Chem. Mater. 15 (2003) p.4149.

[9] J.M. McLellan, Z.Y. Li, A.R. Siekkinen and Y.N. Xia, Nano Lett. 7 (2007) p.1013.

[10] P.N. Njoki, I.S. Lim, D. Mott, H.Y. Park, B. Khan, S. Mishra, R. Sujakumar, J. Luo and C.J. Zhong, J. Phys. Chem. C 111 (2007) p.14664.

[11] R. Aroca, Surface-enhanced Vibrational Spectroscopy, Wiley & Sons, Chichester UK, 2006.

[12] X.Y. Lang, L.Y. Chen, P.F. Guan, T. Fujita and M.W. Chen, Appl. Phys. Lett. 94 (2009) p.213109.

[13] L. Zhang, L. Chen, H. Liu, Y. Hou, A. Hirata, T. Fujita and M.W. Chen, J. Phys. Chem. C 115 (2011) p.19583.

[14] K. Kneipp, Y. Wang, H. Kneipp, L.T. Perelman, I. Itzkan, R. Dasari and M.S. Feld, Phys. Rev. Lett. 78 (1997) p.1667.

[15] S. Nie and S.R. Emory, Science 275 (1997) p.1102.

[16] A. Damin, S. Usseglio, G. Agostini, S. Bordiga and A. Zecchina, J. Phys. Chem. C 112 (2008) p.4932.

[17] A.M. Giovannozzi, F. Rolle, M. Sega, M.C. Abete, D. Marchis and A.M. Rossi, Food Chem. 159 (2014) p.250.

[18] J. Qi, P. Motwani, M. Gheewala, C. Brennan, J.C. Wolfe and W.C. Shih, Nanoscale 5 (2013) p.4105.

[19] W.E. Doering and S. Nie, J. Phys. Chem. B 106 (2002) p.311.

[20] A.P. Budnyk, A. Damin, G. Agostini and A. Zecchina, J. Phys. Chem. C 114 (2010) p.3857.

[21] L. Vigderman and E.R. Zubarev, Langmuir 28 (2012) p.9034.

[22] T.T.B. Quyen, W.N. Su, K.J. Chen, C.J. Pan, J. Rick, C.C. Chang and B.J. Hwang, J. Raman Spectrosc. 44 (2013) p.1671.

[23] X. Lang, L. Qian, P. Guan, J. Zi and M.W. Chen, Appl. Phys. Lett. 98 (2011) p.093701.

[24] L. Zang, X. Lang, A. Hirata and M.W. Chen, ACS Nano 6 (2011) p.4407.

[25] C. Fang, J.G. Shapter, N.H. Voelckerb and A.V. Ellis, RSC Adv. 4 (2014) p.19502.

[26] S. Xu, Y. Yao, P. Wang, Y. Yang, Y. Xia, J. Liu, Z. Li and W. Huang, Int. J. Electrochem. Sci. 8 (2013) p.1863.

[27] J. Weissmueller, R.C. Newman, H.J. Jin, A.M. Hodge and J.W. Kysar, MRS Bulletin 34 (2009) p.557.

[28] X.Y. Lang, P.F. Guan, L. Zhang, T. Fujita and M.W. Chen, J. Phys. Chem. C 113 (2009) p.10956.

[29] M. Moskovitz, J. Raman Spectrosc. 36 (2005) p.485.

[30] S. Van Petegem, S. Brandstetter, R. Maass, A.M. Hodge, B.S. El-Dasher, J. Biener, B. Schmitt, C. Borca and H. Swygenhoven, Nano Lett. 9 (2009) p.1158.

[31] F. Scaglione, P. Rizzi and L. Battezzati, J. Alloys Compd. 536S (2012) p.S60.

[32] P. Rizzi, F. Scaglione and L. Battezzati, J. Alloys Compd. 586S (2014) p.S117.

[33] E.M. Paschalidou, F. Scaglione, A. Gebert, S. Oswald, P. Rizzi and L. Battezzati, J. Alloys Compd. (2015).

[34] Y. Wan, X. Wang, S. Liu, Y. Li, H. Sun and Q. Wang, Int. J. Electrochem. Sci. 8 (2013) p.12837.

[35] Z.X. Liang, T.S. Zhao, J.B. Xu and L.D. Zhu, Acta 54 (2009) p.2203.

[36] M. Grden, M. Lukaszewski, G. Jerkiewicz and A. Czerwinski, Electrochim. Acta 53 (2008) p.7583.

[37] Y.Y. Yang, J. Ren, H.X. Zhang, Z.Y. Zhou, S.G. Sun and W.B. Cai, Langmuir 29 (2013) p.1709.

[38] L.Y. Chen, J.S. Yu, T. Fujita and M.W. Chen, Adv. Funct. Mater. 19 (2009) p.1221.

[39] H. Guo, L. Ding and Y. Moa, J. Mol. Struct. 991 (2011) p.103.

[40] O. Blajiev, H. Terryn, A. Hubin, L. Soukupova and P. Geerlings, J. Raman Spectrosc. 37 (2006) p.777.

[41] L. Battezzati, I. Moiraghi, I. Calliari and M. Dabalà, Intermetallics 12 (2004) p.327.

[42] S.W. Joo, Vibr. Spectrosc. 34 (2004) p.269.